Science Advances

AAAS

advances.sciencemag.org/cgi/content/full/3/2/e1600922/DC1

Supplementary Materials for

Two billion years of magmatism recorded from a single Mars meteorite ejection site

Thomas J. Lapen, Minako Righter, Rasmus Andreasen, Anthony J. Irving, Aaron M. Satkoski, Brian L. Beard, Kunihiko Nishiizumi, A. J. Timothy Jull, Marc W. Caffee

Published 1 February 2017, *Sci. Adv.* **3**, e1600922 (2017)
DOI: 10.1126/sciadv.1600922

This PDF file includes:

- Supplementary Materials and Methods
- fig. S1. Images of the outer and inner portions of NWA 7635.
- fig. S2. Plots of chondrite-normalized trace element compositions of shergottites and NWA 7635.
- fig. S3. Measured μ^{142}Nd values for fractions of NWA 7635, Himalayan garnet schist 1, and Himalayan garnet schist 2 versus ^{142}Ce interference on ^{142}Nd, ^{144}Sm interference on ^{144}Nd, and the spike-to-sample ratio.
- table S1. List of samples and data sources for source composition calculations.
- table S2. ^{147}Sm-^{143}Nd isotopic analyses of NWA 7635.
- table S3. Descriptions and weights of NWA 7635 samples analyzed for radiogenic and cosmogenic isotopes.
- table S4. Laser ablation ICP-MS compositions of primary mineral phases in NWA 7635.
- table S5. ^{146}Sm-^{142}Nd isotopic analyses of NWA 7635.
- table S6. Lu-Hf isotopic analyses of NWA 7635.
- table S7. Rb-Sr isotopic analyses of NWA 7635 maskelynite.
- References (*42–78*)

Supplementary Materials and Methods

1: Major element compositions of constituent mineral phases

Olivine, pyroxene and plagioclase (maskelynite) in NWA 7635 were analyzed by electron-probe microanalysis by S. Kuehner, University of Washington. The specimen is porphyritic with phenocrysts (up to 200μm) of plagioclase completely converted to maskelynite ($An_{60.7\text{-}61.8}$), ferroan olivine ($Fa_{56.3–60.6}$; FeO/MnO = 42−49), augite ($Fs_{28.5\text{-}29.7}Wo_{32.3\text{-}33.8}$; FeO/MnO = 29-38; TiO_2 = 0.24 wt.%; Cr_2O_3 = 0.93 wt.%), and low Ti magnetite in a much finer grained matrix composed mainly of Fe-rich augite ($Fs_{74.8\text{-}77.2}Wo_{21.8\text{-}23.8}$; FeO/MnO = 45−48). Accessory pyrrhotite and rare ilmenite are present, but no identifiable phosphate grains have been found. The calculated number of Fe3+ cations per 4 total cations in clinopyroxene is 0.00 – 0.07. Major element concentrations, in weight percent, of olivine, clinopyroxene, and maskelynite are listed below:

	Olivine			Clinopyroxene				Maskelynite	
SiO_2	34.22	33.37	34.21	‡ 50.18	‡ 50.75	† 44.35	† 45.95	53.33	53.84
TiO_2	--	--	--	0.21	0.27	1.02	0.88	b.d.l.	b.d.l.
Al_2O_3	--	--	--	1.58	2.36	1.30	0.95	29.42	28.8
Cr_2O_3	0.19	0.14	0.14	0.95	1.14	0.06	0.07	b.d.l.	b.d.l.
FeO	44.63	47.12	45.95	17.41	16.94	41.93	40.17	0.59	0.51
MnO	1.07	0.96	1.06	0.46	0.58	0.86	0.88	b.d.l.	b.d.l.
MgO	19.42	17.19	16.83	13.42	12.54	0.32	0.43	b.d.l.	b.d.l.
NiO	0.03	0.07	0.05	--	--	--	--	--	--
CaO	0.44	0.60	1.16	15.37	15.10	9.25	9.98	12.9	12.1
SrO	--	--	--	--	--	--	--	0.03	b.d.l.
Na_2O	--	--	--	0.17	0.18	0.12	0.06	4.4	4.28
K_2O	--	--	--	--	--	--	--	0.02	b.d.l.
SUM	100.00	99.45	99.40	99.75	99.86	99.21	99.37	100.69	99.53

-- not measured; b.d.l. below detection limit; ‡ augite; † Fe-rich augite

2: Bulk composition and oxygen isotopes

Northwest Africa (NWA) 7635 is a 196 gram fresh shergottite meteorite (fig. S1). Powder ground from a 1.1 gram interior slice was analyzed by X-ray fluorescence (XRF) and quadrupole inductively-coupled plasma mass spectrometry (ICP-MS) for major and

trace element concentrations by R. Conrey, Washington State University and G. Chen, University of Alberta. Major element concentrations, in weight percent, are:

SiO_2	TiO_2	Al_2O_3	Cr_2O_3	FeO	MnO	MgO	CaO	Na_2O	K_2O	P_2O_5
47.55	0.61	11.16	0.15	22.49	0.47	4.11	9.77	2.18	0.07	0.28

Trace element compositions are: Ni 7.7, V 40.4, Rb 0.40, Sr 69.2, Zr 9.8, Ba 9.9, La 0.19, Ce 0.83, Pr 0.196, Nd 1.38, Sm 0.85, Eu 0.33, Gd 1.65, Tb 0.36, Dy 2.57, Ho 0.62, Er 1.91, Tm 0.289, Yb 1.99, Lu 0.30, Hf 0.30, Pb 0.93, Th 0.13 (all in ppm). The bulk Mg/(Mg+Fe) ratio of 0.25 is relatively low and nearly identical to that of Los Angeles. The highly evolved composition of NWA 7635 indicates that its parental magma likely underwent significant fractionation. The rare earth element (REE) abundances of NWA 7635 give a similar pattern to those of other depleted shergottites with a strong depletion in light REEs (low chondrite-normalized La/Lu ratios) (fig. S2).

The oxygen isotope composition of NWA 7635 is reported in the Meteoritical Bulletin Database (http://www.lpi.usra.edu/meteor/metbull.php?code=56618). The reported compositions are: $\delta^{17}O$ = 2.536, 2.521, 2.513; $\delta^{18}O$ = 4.241, 4.220, 4.217; $\Delta^{17}O$ = 0.297, 0.294, 0.287 (for a TFL slope of 0.528; K. Ziegler, UNM) for three acid washed subsamples analyzed by laser fluorination.

3: In situ trace element analyses of constituent phases

Trace element abundances in constituent phases of NWA 7635 were determined by laser ablation inductively coupled plasma mass spectrometry (LA-ICP-MS) at the University of Houston on a representative thick section of NWA 7635. Analyses were performed using a 193 nm wavelength PhotonMachines Analyte.193 laser ablation system coupled to a Varian 810-MS quadrupole ICP-MS. Prior to laser analysis, the major elements abundances were determined by electron probe microanalysis (EPMA) at the NASA Johnson Space Center. During LA-ICP-MS analyses, the following isotopes were measured: ^{25}Mg, ^{26}Mg, ^{29}Si, ^{31}P, ^{39}K, ^{43}Ca, ^{45}Sc, ^{49}Ti, ^{51}V, ^{53}Cr, ^{55}Mn, ^{59}Co, ^{62}Ni, ^{65}Cu, ^{66}Zn, ^{71}Ga, ^{72}Ge, ^{85}Rb, ^{86}Sr, ^{89}Y, ^{90}Zr, ^{93}Nb, ^{118}Sn, ^{137}Ba, ^{139}La, ^{140}Ce, ^{141}Pr, ^{146}Nd, ^{147}Sm,

^{151}Eu, ^{157}Gd, ^{159}Tb, ^{161}Dy, ^{165}Ho, ^{167}Er, ^{169}Tm, ^{172}Yb, ^{175}Lu, and ^{178}Hf. For each analyzed spot (50–100 μm in diameter), we measured a 15–20 second gas blank prior to sample ablation. Samples were ablated for 20–30 seconds at a laser power of ~3 mJ and a 4 ns pulse at a repetition rate of 10 Hz. All trace element data were corrected for laser and ICP-MS elemental fractionation with internal elements Si and Mg calibrated by EPMA and the USGS external standard BHVO-2G glass using the commercial data reduction software package Glitter. The USGS SRM BIR-1G glass standard was used to monitor external reproducibility and instrument drift. Representative trace element concentrations of the major silicate phases are presented in table S4 and fig. S2. The bulk rock and mineral compositions show depletion in LREE with an increasing slope from LREE to MREE and a near flat pattern from the MREE to HREE. A positive Eu anomaly is observed in plagioclase, whereas olivine, pyroxene and bulk rock have small negative Eu anomalies. The relatively high light REE and other incompatible element (e.g. Rb) concentrations in olivine suggest that melt inclusions dominated the trace element abundances for the olivine analyses.

4: Sample preparation for isotopic studies

Three intact pieces of NWA 7635 totaling 2.2g were used for isotope analyses. Prior to crushing, these three pieces were washed in an ultrasonic bath for 5 minutes with ultrapure H_2O to remove any surficial contamination. All three pieces were crushed by hand with an alumina mortar and pestle dedicated to extraterrestrial materials. A 1.1 g piece was crushed into a powder and used for bulk analysis (sample F1, tables S1 and S2). Two other pieces (total of 1.1 g) were crushed and sieved into >325 mesh (<44 μm) and 200−325 mesh (44−75 μm). Two fractions were then separated from >325 mesh size and used for Sm-Nd and Pb-Pb (reported elsewhere) by sequential dissolution (sample F3) and Sm-Nd bulk analysis (sample F4). Mineral separations were attempted on the 200-325 mesh fractions. A plagioclase fraction (sample F5) was separated by hand-picking. Due to the very fine-grained nature of NWA 7635, this only yielded ~3.7 mg of clean maskelynite and this fraction was used for Rb-Sr isotope analysis. No Sm-Nd, Lu-Hf, or Pb-Pb analyses were attempted on this fraction due to its small size. The remainder of the 200−325 mesh fraction contained significant quantities of plagioclase/maskelynite as the

typical grain size of the quenched matrix in NWA 7635 is smaller than finest mesh size (325 mesh; 44 μm). The remainder of the 200−325 mesh fraction was separated using Frantz magnetic separator in 0.02 A intervals starting at 0.02 A. From this, olivine-rich (sample F6) and pyroxene-rich (sample F7) sample fractions were separated. Due to the abundance of composite grains resulting from the fine-grained nature of the sample, no further hand separation was done on these fractions. The cosmogenic nuclide concentration measurements were conducted on a separate bulk rock fraction (sample F2).

Sample F1 was weighed and mixed ^{176}Lu-^{178}Hf and ^{149}Sm-^{150}Nd spikes were added prior to digestion. This sample was not leached to avoid decoupling of Lu and Hf. The F4, F6, and F7 samples were weighed and gently leached for 10 minutes with 1.0 M HCl at room temperature. After the dilute HCl leaching, the residues were washed 3 times with ultrapure H_2O, which were added to the leachate fractions. Both leachates and residues were dried resulting in the samples L and R, respectively. Prior to digestion, mixed ^{149}Sm-^{150}Nd and ^{87}Rb-^{84}Sr spikes were added to samples L4, L6, L7, R4, R6 and R7. The F3 sample fraction was dissolved by sequential dissolution, first by ultrasonification three times in 0.5 M HNO3 for 10 minutes (F3-L1), followed by leaches with room temperature leach 1.0 M HCl (F3-L2), warm 6 M HCl (F3-L3), room temperature 6 M HCl – 0.2 M HF (F3-L4), warm 6 M HCl – 2 M HF (F3-L5), and a final step of 7 M HNO3 – 14 M HF (F3-L6) after which the sample was completely dissolved. A mixed ^{149}Sm-^{150}Nd spike was added to all six fractions from the sequential dissolution prior to sample digestion.

The general dissolution and digestion scheme is as follows: 1) hotplate digestion in 29 M HF in Teflon beakers to facilitate the breakdown of the majority of the silicates, 2) hotplate digestion in 8:1 HF:HNO_3 to dissolve the remaining minerals, 3) hotplate digestion with 7M HNO_3 to remove insoluble fluorides, and 4) repeated dissolution with 8M HCl until the sample solutions were clear and no solids are detected after centrifuging. In between each step, the sample solutions were taken to dryness, generally at 100°C. Following the final dry down, the samples were re-dissolved in 6.0 M HCl for Lu-Hf, Sm-Nd, and Rb-Sr column chemistry.

Sample F1 was separated using a four-column procedure to separate Sm, Nd, Lu, and Hf, beginning with Fe removal via anion exchange (AG1X8 200–400 mesh resin) in HCl, then isolation of Hf using Eichrom Ln-spec resin, followed by isolation of the REE via RE-spec resin, and concluding with isolation of Lu, Sm, and Nd with AG50W-X4 200–400 mesh resin in NH_4-form with α-hydroxyisobutyric Acid (α-HIBA). Sample F4, F6, and F7 were separated using a four-column procedure to separate Rb, Sr, Sm, and Nd, beginning with Rb, Sr, and REE isolation via cation exchange, followed by Sm–Nd purification using α-HIBA, and Rb and Sr clean-up columns for the Rb and Sr fractions, respectively using BioRad AG MP-50 resin for Rb, and Eichrom Sr-spec resin for Sr. Sample F3 was separated using a four-column procedure to separate Pb, Sm, and Nd, beginning with anion exchange chemistry in HBr to separate Pb and matrix, followed by a clean-up anion HBr column for the Pb fraction and cation and α-HIBA columns to separate Sm and Nd from the matrix fraction, using the same steps as for the Sm-Nd fractions of samples F4, F6, and F7. Sample F5 was separated using a three-column procedure to separate Rb and Sr, using the same procedure as for the Rb-Sr fractions of samples F4, F6, and F7. For details of the chemical separation procedures see (*35*), (*36*), and (*42*). Total procedural blanks are <50pg, <15pg, <40pg, <17 pg, <15pg, 400pg, for Nd, Sm, Hf, Lu, Rb, and Sr, respectively.

5: Mass Spectrometry

5.1 Sm-Nd

All Sm, Nd, Lu and Hf isotope analyses were carried out at University of Houston using a Nu Instruments NuPlasma II MC-ICP-MS. For Nd isotope analyses, the seven stable isotopes of Nd: ^{142}Nd, ^{143}Nd, ^{144}Nd, ^{145}Nd, ^{146}Nd, ^{148}Nd, and ^{150}Nd were analyzed as well as ^{140}Ce, ^{147}Sm, and ^{149}Sm which are used to monitor, and ultimately correct for, isobaric interferences on ^{142}Nd (Ce), ^{144}Nd (Sm), ^{148}Nd (Sm), and ^{150}Nd (Sm). Standards and samples were measured in solutions of 10–100 ppb and were introduced into the mass spectrometer through an Aridus II desolvating nebulizer fitted with a 50 μl/min self-aspirating PFA teflon nebulizer. Throughout the Nd isotope analysis of samples, the JNdi-1 Nd standard was used to correct for instrumental fractionation. UH Ames Nd and

Caltech Nd were analyzed as unknown standards. The mean value of JNdi-1, UH Ames Nd, and Caltech Nd standards during the sample analyses are $^{143}Nd/^{144}Nd = 0.512115 \pm 26$ (2 SD, n = 27), and $^{143}Nd/^{144}Nd = 0.511899 \pm 18$ (2 SD, n = 9), and $^{143}Nd/^{144}Nd = 0.511988 \pm 30$ (2 SD, n = 9) respectively. Samarium isotope analyses followed procedures in (*35, 42*). External reproducibility in $^{143}Nd/^{144}Nd$ and $^{147}Sm/^{144}Nd$ ratios are 0.0046% and 0.2% (2σ), respectively, and these values are used as the measurement uncertainty. The ^{147}Sm-^{143}Nd data are presented in table S1.

With an age of 2.4±0.1 Ga, NWA 7635 formed long after the effectively complete decay of short-lived ^{146}Sm; the measured $^{142}Nd/^{144}Nd$ ratio of NWA 7635 is inherited from the magma sources. The $^{142}Nd/^{144}Nd$ ratios of the individual mineral fractions, leachates, and residues are expected to be identical, therefore the individual short (~7 minute) analysis by MC-ICP-MS can be treated like individual block analyses from a long Thermal Ionization Mass Spectrometer (TIMS) analysis and averaged in the same way to get a reasonably precise and accurate measurement of the $^{142}Nd/^{144}Nd$ ratio of NWA 7635. Drift in amplifier gains and detector efficiencies are corrected through the sample-standard bracketing approach between each analysis (*35*) eliminating the need to analyze Nd with dynamic-multicollection or multi-static methods. The advantage of this approach is that it allows measurement of both $\mu^{142}Nd$ and ^{147}Sm-^{143}Nd systematics on the same sample aliquots, with a total amount of Nd analyzed equivalent to that of a high-precision ^{142}Nd analyses by TIMS, without the requirement of measuring it on a sample aliquot dedicated for this one measurement.

The $\mu^{142}Nd$, $\mu^{145}Nd$, ^{142}Ce interference, ^{144}Sm interference, spike/sample ratio, and amount of sample used for NWA 7635, two enriched shergottites, two very young terrestrial garnet schists from the Himalayas assumed not to have an inherited ^{142}Nd anomaly, and normal standards are presented in table S5. The instrumental mass and elemental fractionations in the MC-ICP-MS plasma source are very stable as demonstrated by the low uncertainties in the Ce and Sm isobar corrections (table S5). Although the isobar corrections can be as high as 500 ppm, there are no systematic biases in the data for the terrestrial samples whose $\mu^{142}Nd$ is known to be zero or in the data for

the shergottites (fig. S3). This allows for the determination of μ^{142}Nd on samples passed through the Nd separation chemistry once, thus maintaining a very high yield (>95%) and measurements utilizing smaller sample sizes. Cerium and Samarium interferences reported here are comparable to those reported from TIMS analyses (e.g. *43*); fig. S3 shows that there is no variation in measured μ^{142}Nd with Ce and Sm interference levels. Spike subtraction for the μ^{142}Nd measurements follows the procedures of (*35*), the high ^{150}Nd/^{142}Nd ratio of the spike (238.50) yields a minimal correction, fig. S3 shows that there is no correlation in measured μ^{142}Nd with the spike to sample ratio.

The Himalayan garnet schists (garnet schists #1 and #2), give μ^{142}Nd values of 0.0±9.9 and +0.8±6.0, respectively. For garnet schist #2, a large amount of sample was deliberately consumed to investigate if large sample sizes would lead to improved precision, which it only does slightly and not proportionally to sample size. The measured zero μ^{142}Nd values for the garnet schists suggest that the measurements are accurate and not biased by Ce or Sm interferences or the spike subtraction. All samples have μ^{145}Nd values within error of zero and there is no correlation between measured μ^{142}Nd and μ^{145}Nd with spike/sample ratio indicating that the spike subtraction doesn't add significant analytical bias to the measured μ^{142}Nd values. Preliminary values for enriched shergottites NWA 6963 (whole rock only) and LAR 12011 give μ^{142}Nd values of -17.7±7.0 and -14.1±6.3, respectively. These are indistinguishable from values reported for enriched shergottites by (*13*) and (*44*), lending further credence to the measured μ^{142}Nd value for NWA 7635 being accurate. Further details, including ^{147}Sm-^{143}Nd data for NWA 6963 and LAR 12011 are given in (*45*) and (*46*), respectively.

Whereas the precision of the MC-ICP-MS ^{142}Nd analyses is slightly worse than that reported for recent TIMS analyses (*43*, *13*), the very stable instrumental mass and elemental fractionations in the MC-ICP-MS source avoids some of the analytical challenges observed for TIMS analyses (*47*, *48*). In particular, this approach eliminates the need to aliquot samples specifically for ^{142}Nd analyses, thus reducing sample sizes required for combined ^{147}Sm-^{144}Nd chronology and ^{142}Nd/^{144}Nd isotope tracer studies on an single meteorite.

5.2 Lu-Hf

During Hf isotope analysis, the following isotopes were analyzed: ^{174}Hf, ^{176}Hf, ^{177}Hf, ^{178}Hf, ^{179}Hf and ^{180}Hf as well as ^{171}Yb, ^{172}Yb, ^{173}Yb, ^{175}Lu, ^{181}Ta and ^{182}W which will be used to monitor, and ultimately correct for, isobaric interferences on ^{174}Hf (Yb), ^{176}Hf (Yb and Lu) and ^{180}Hf (Ta and W). Instrumental mass fraction correction and spike striping followed methods of (*35*). Standards and samples were measured in solutions of 10–50 ppb and were introduced into the mass spectrometer through an Aridus II desolvating nebulizer fitted with a 50 μl/min self-aspirating nebulizer. Throughout Hf isotope analysis of samples, the UH JMC 475 Hf standard was used to correct for instrumental fractionation. A different aliquot of JMC 475 Hf (Wisconsin = USGS) with a slightly different isotopic composition from the UH JMC 475 was analyzed as an unknown standard in addition to a Teledyne Hf standard. Repeated analysis of the Hf standard JMC-475 (UH) yielded ^{176}Hf/^{177}Hf = 0.282196 ± 9 (2σ, n = 18), JMC-475 (Wisconsin/USGS) yielded ^{176}Hf/^{177}Hf = 0.282176 ± 7 (2σ, n = 3), and Teledyne Hf yielded ^{176}Hf/^{177}Hf = 0.282015 ± 8 (2σ, n = 3). Lutetium isotope analyses followed procedures (*35*). The external reproducibility in ^{176}Hf/^{177}Hf and ^{176}Lu/^{177}Hf ratios are 0.0035% and 0.2% (2σ), respectively, and these values are used as the measurement uncertainty. The Lu-Hf data are presented in table S6.

5.3 Rb-Sr

All Rb and Sr isotope analyses were performed at the University of Wisconsin-Madison using a Micromass Sector 54 thermal ionization mass spectrometer. Strontium isotope analyses were done using Re filaments with a TaF activator, following the loading methods outlined in (*49*) and a multi-collector three-jump dynamic analysis with internal exponential normalization to an ^{86}Sr/^{88}Sr value of 0.1194. The reported uncertainties for the ^{86}Sr/^{88}Sr ratio are the 2-SE determined by in-run statistics. Repeat analysis of 10ng Sr loads of NIST SRM-987 Sr isotope standard ran during the same period as the samples were analyzed yielded an average ^{87}Sr/^{86}Sr value of 0.710266 ± 17 (2 SD, n = 46). Analyses of Rb were done using a multi-Faraday collector static routine. The weighted average ^{87}Rb/^{85}Rb ratio of 10 analyses of NIST SRM-984 was 0.3858 ± 30 (2 SD; n=7).

Based on replicate analysis of Rb and Sr standards, the $^{87}Rb/^{84}Sr$ ratio is precise to ±0.8%. Rubidium-strontium isotope data for sample F5 are listed in table S7.

6: Cosmogenic radionuclide analyses

To eliminate weathering products, a chip of sample was etched with a 0.2 N HNO_3 solution in an ultrasonic bath for 10 minutes. After acid leaching, 81.8 mg of NWA 7635 was dissolved in an HF-HNO_3 mixture along with Be and Cl carriers. After taking an aliquot for chemical analysis by ICP-OES, Be, Al, Cl, and Mn were chemically separated and purified for AMS measurements. The AMS measurements for these nuclides were performed at the PRIME lab, Purdue University. A small (~60mg) fragment of NWA 7635 was measured at the Accelerator Mass Spectrometry Laboratory of the University of Arizona in Tucson, AZ, to determine the terrestrial residence age using ^{14}C. The sample was cleaned in 85% phosphoric acid to remove weathering products and then fused with Fe chips in a radio-frequency induction furnace in an oxygen flow to release CO_2 gas. The gas was then reduced to graphite, pressed into a target holder and analyzed for ^{14}C by accelerator mass spectrometry. The terrestrial age is calculated to be 2.3±1.3 kyr based on ^{14}C, assuming a saturated activity of 61 dpm/kg for shergottites (*50*).

The measured concentrations were ^{10}Be 9.7±0.1 dpm/kg, ^{26}Al 70±5 dpm/kg, and ^{14}C 46±1 dpm/kg. The exposure age in space is 1.0±0.1 Myr, based on the chemical composition of the measured sub-sample (2.28 % Mg, 5.49 % Al, 6.06 % Ca, 3100 ppm Mn, and 16.4 % Fe) and model production rates. Although the recovered mass is small, the pre-atmospheric radius is estimated to be ≥20 cm based on our cosmogenic nuclide measurements.

7: Mantle source composition calculations

Epsilon notation, for example $\varepsilon^{176}Hf_{CHUR}$, = ($^{176}Hf/^{177}Hf_{sample}/^{176}Hf/^{177}Hf_{CHUR}$ − 1)*10,000; CHUR refers to Chondritic Uniform Reservoir model values (see below) for the Lu-Hf, as well as Sm-Nd, isotope systems.

The source $^{176}Lu/^{177}Hf$, $^{147}Sm/^{144}Nd$, and $^{87}Rb/^{86}Sr$ ratios are calculated following (*2*, *6*) assuming a chondritic bulk Mars for the lanthanides and Hf and a $^{87}Rb/^{86}Sr$ ratio of 0.28 (*36*), a planet formation age (T_0) of 4567 Ma, a source differentiation (T_1) age of 4504 Ma, and CHUR parameters of $^{176}Lu/^{177}Hf = 0.0336$ (*51*), $^{176}Hf/^{177}Hf_{4567\ Ma} = 0.279825$, λ-$^{176}Lu = 1.865 \times 10^{-11}\ y^{-1}$, $^{147}Sm/^{144}Nd = 0.1967$, $^{143}Nd/^{144}Nd_{4567\ Ma} = 0.506674$, λ-$^{147}Sm = 6.54 \times 10^{-12}\ y^{-1}$, $^{87}Rb/^{86}Sr = 0.28$, $^{87}Sr/^{86}Sr_{4567\ Ma} = 0.69899$, and λ-$^{87}Sr = 1.40 \times 10^{-11}\ y^{-1}$. The source $^{176}Lu/^{177}Hf$ ratio of NWA 7635 is calculated from the age-corrected bulk rock analysis (F1), the source $^{87}Rb/^{86}Rb$ ratio of NWA 7635 is calculated from the age-corrected maskelynite residue analysis (F5-R). Data sources for the time of crystallization (T_2) and initial isotopic composition are listed in table S3.

8: Sm-Nd age calculations

Samarium-neodymium isotope data used for the age calculations are listed in table S1. The final age calculation using a ^{147}Sm decay constant of $6.54 \times 10^{-12}\ y^{-1}$, isochron regression software IsoPlot (v.3.76), and sample fractions whole rock F1, WR3-L3, WR4-R, olivine-R, pyroxene-R, weak acid leachates (n=4), and HF stepwise dissolution samples (n=3) (tables S1 and S2) resulted in an igneous crystallization age of 2403 ± 140 Ma (MSWD = 5.1). The calculated age based on unleached whole rock F1, WR4-R, olivine-R, and pyroxene-R fractions is 2444 ± 440 Ma, an identical, but lower precision age calculation due the limited spread in Sm/Nd ratios than the age calculation including the leachates.

Due to the overall fine-grained texture of the sample where most phenocrysts are < 200 μm and most finely-intergrown groundmass grains are < 50 μm across (Fig. 1), chemical leaching with HCl solutions was applied to remove more labile materials, such as phosphate, in order to increase the spread in Sm/Nd ratios of the digested and analyzed samples. This is an approach commonly and successfully used for Sm-Nd isotope analyses of shergottites because there is little evidence for decoupling of radiogenic $^{143}Nd/^{144}Nd$ ratio from the measured $^{147}Sm/^{144}Nd$ ratio of residues and leachates during washing in HCl (e.g. 14, 18, 29). This approach is also useful for removing surface contamination and weathering products such as carbonate. Because the Sm-Nd isotope

data for NWA 7635 leachates lie on the 2.4 Ga isochron defined by the unleached whole rock (F1) and mineral residues, there is no evidence in the Sm-Nd data that there is a contaminant component in the HCl leachates. Although no distinct phosphate minerals were observed in the sample, the relatively low $^{147}Sm/^{144}Nd$ ratios of the leachates for this sample (0.3056 - 0.3163) point to HCl soluble materials, such as phosphate, hosting much of the REE in these fractions (e.g. *52*). Since the leachates represent a single Sm-Nd reservoir likely dominated by phosphate minerals, we combined these data into a single point (*53*) so as not to over-represent the low Sm/Nd ratio fraction in the isochron calculations. Age calculations which include the HCl leachates as separate data points yields an age of 2333 ± 80 Ma (MSWD = 7.5), within error of, but more precise than our preferred age. We prefer the lower precision and likely more representative age of 2403 ± 140 Ma.

Through our sample processing procedure for analyses of Pb isotopes (not reported here), we also applied a more rigorous sequential digestion procedure for whole rock sample F3 using variable mixtures of HCl, HF, and HNO_3 (samples F3-L4, L5, and L6; see section 4 and tables S1 and S2) and analyzed these fractions for their Sm and Nd isotopic compositions. The use of HF during sequential or partial dissolution has the potential to fractionate Sm/Nd ratios in some USGS standard materials by as much as 2% (*54*). For samples F3-L4, L5, and L6, the slope defined by their $^{147}Sm/^{144}Nd$ and $^{143}Nd/^{144}Nd$ ratios is shallower than the slope defined by all of the other phases. This can either be a result of open-system behavior during terrestrial and/or Martian weathering or decoupling between $^{147}Sm/^{144}Nd$ and $^{143}Nd/^{144}Nd$ ratios during the dissolution process. This was tested by reintegrating these samples (whole Rock HF step-wise dissolution in tables S1 and S2). If the system was open, then the integrated data would not plot on the isochron defined by the other points. These integrated data, however, do lie on the isochron and are included in the final age calculation which is based on all of the measured Sm-Nd data without exclusion.

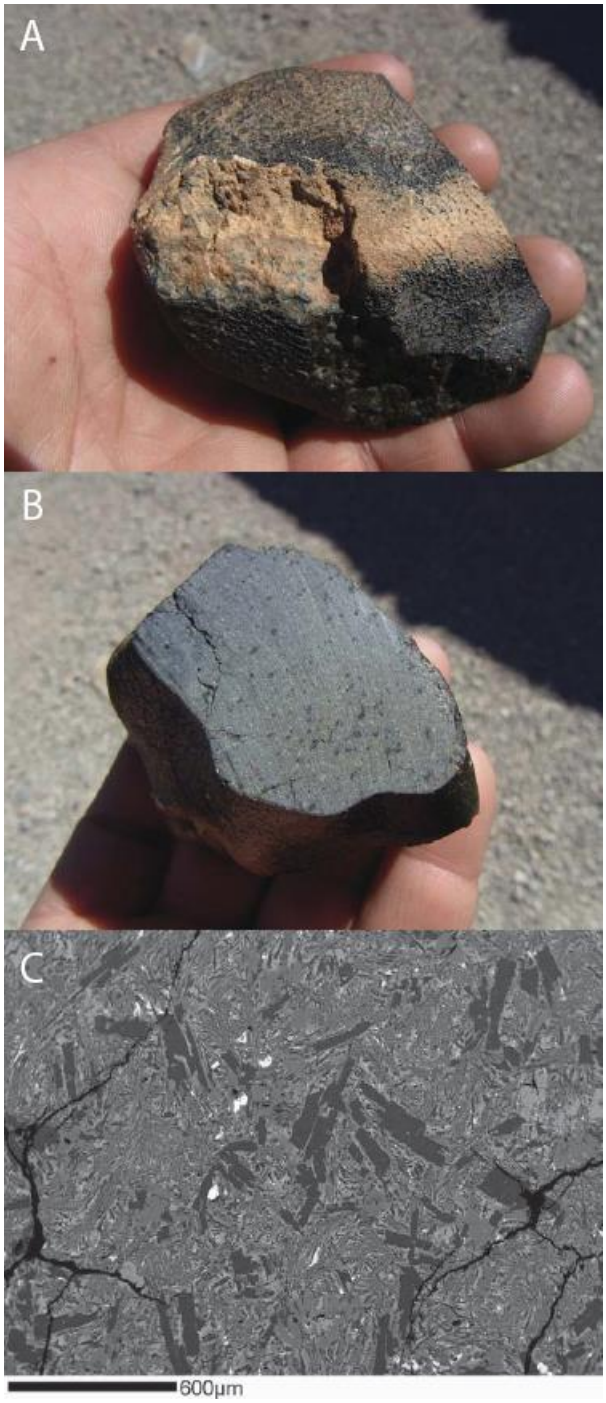

fig. S1. Images of the outer and inner portions of NWA 7635.

Hand sample images of the cut NWA 7635 stone (fig. S1a, b) and a representative back-scattered electron image of the igneous texture of the stone (fig. S1c). In fig. S1c, note the large maskelynite phenocrysts (dark gray) hosted by a groundmass of composed mainly

of olivine (medium gray) with magnetite and pyrrhotite (bright) and pyroxene. Photo credits Mohammed Hmani (**A**, **B**), Scott Kuehner (**C**).

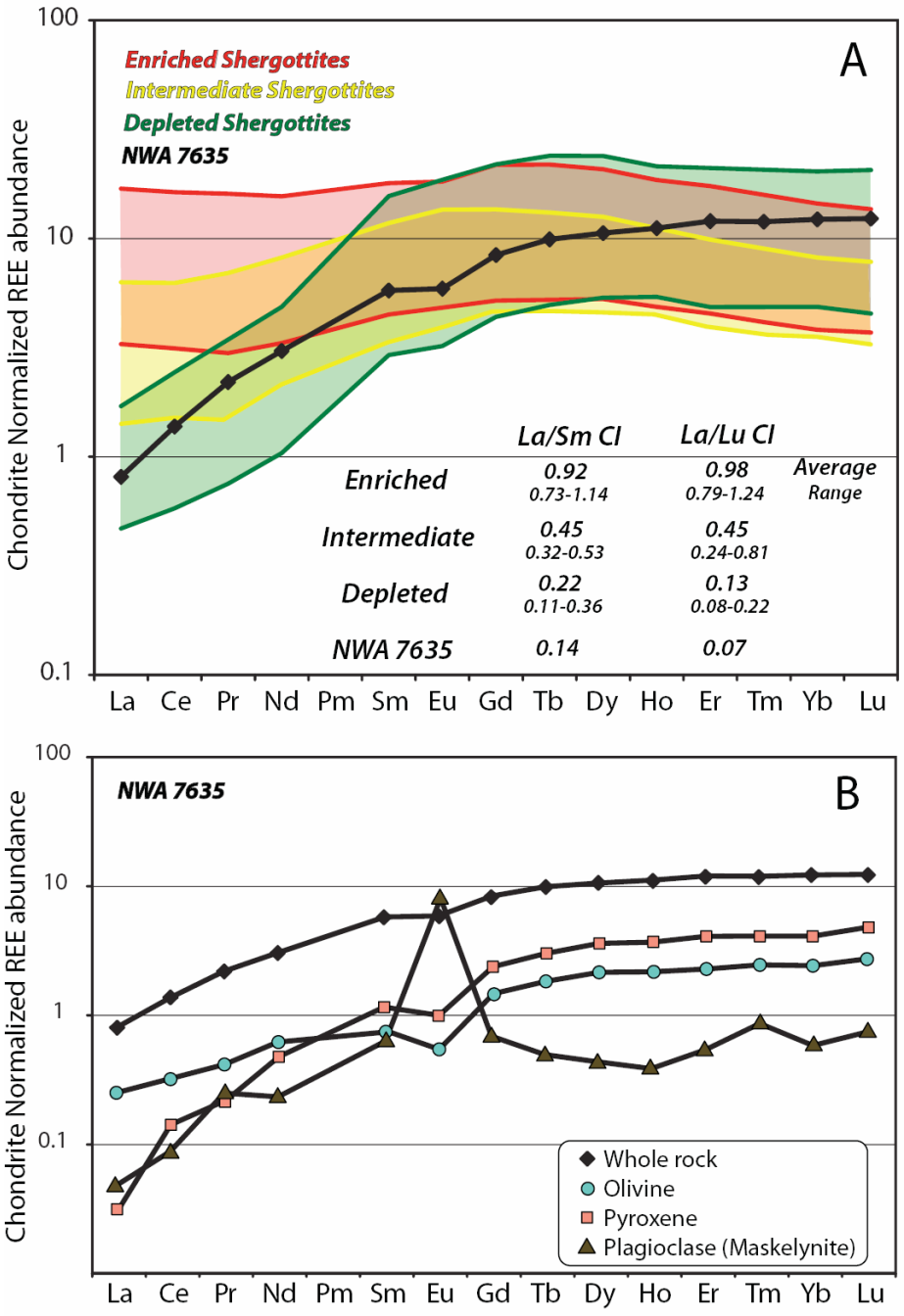

fig. S2. Plots of chondrite-normalized trace element compositions of shergottites and NWA 7635.

Figure S2a shows chondrite-normalized rare earth element concentration data for NWA 7635 whole rock (sample fraction F1) designated by the black diamonds. Pooled data arrays for enriched, intermediate, and depleted shergottites are also shown for reference. Calculated average La/Sm and La/Lu ratios are also shown for reference. Figure S2b

shows chondrite-normalized rare earth element concentration data for the mineral phases in the rock.

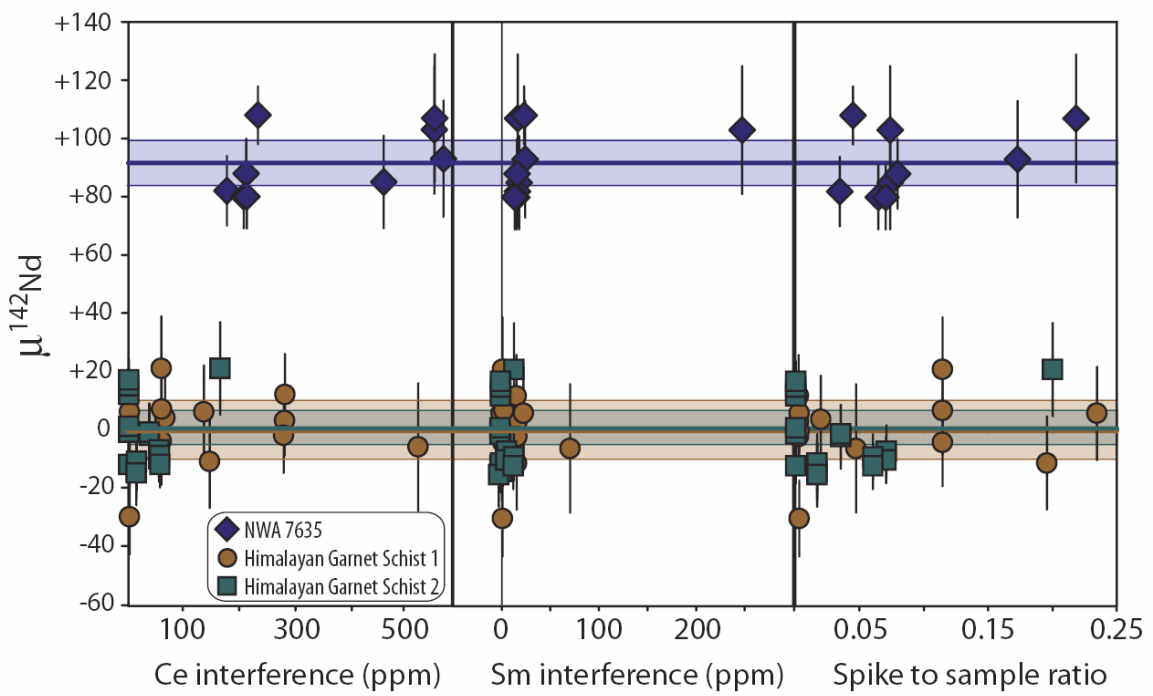

fig. S3. Measured μ^{142}Nd values for fractions of NWA 7635, Himalayan garnet schist 1, and Himalayan garnet schist 2 versus ^{142}Ce interference on ^{142}Nd, ^{144}Sm interference on ^{144}Nd, and the spike-to-sample ratio. The interference and spike levels are comparable for the three samples and are not correlated with the measured μ^{142}Nd values. The absence of correlations suggest that the interference corrections and spike subtraction applied to the data are not introducing analytical artefacts to the dataset within the range of interferences and spike levels measured.

table S1. List of samples and data sources for source composition calculations.

		Source Parent-Daughter Ratios									Data
Sample	Type	$^{147}Sm/^{144}Nd$	Plus	Minus	$^{87}Rb/^{86}Sr$	Plus	Minus	$^{176}Lu/^{177}Hf$	Plus	Minus	Sources
ALH 77005	IS	0.2140	9	9	0.1769	2	2	0.0439	2	2	*13, 15, 57*
ALH 84001	OPX	0.1708	76	89	0.5904	265	245	0.0173	43	50	*12, 58, 59*
DaG 476	DS	0.2640	33	34				0.0510	2	2	*13, 23*
Dhofar 019	DS	0.2679	13	14	0.0508	12	12	0.0491	4	4	*22, 60*
Dhofar 378	ES	0.1852	1	1	0.3432	21	20				*61*
EETA 79001B	IS	0.2263	10	10	0.2128	6	7	0.0442	2	2	*62*
GRV 99027	IS	0.2184	10	10	0.1782	8	8				*63*
LAR 06319	ES	0.1835	6	6	0.3639	15	30	0.0272	1	1	*64, 65*
LEW 88516	IS	0.2113	3	3	0.1768	10	10				*18*
Los Angeles	ES	0.1857	6	6	0.3473	17	17	0.0279	2	2	*13, 66, 67*
NWA 1460	IS	0.2168	24	24	0.1620	14	14				*68, 69*
NWA 856	ES	0.1861	3	6	0.3643	58	57	0.0279	1	1	*13, 70*
NWA 1068	ES	0.1842	17	17	0.3697	14	14				*71*
NWA 2990	IS	0.2068	14	15				0.0411	3	3	*72*
NWA 4468	IS	0.1842	6	6				0.0273	1	1	*72*
NWA 5990	DS	0.2762	8	9	0.0383	3	3				*73*
NWA 7635	DS	0.3035	52	59	0.0228	19	21	0.0594	39	45	*this study*
QUE 94201	DS	0.2827	24	24	0.0330	3	5	0.0502	2	2	*6,57*
RBT 04262	ES	0.1848	29	29	0.3746	11	12	0.0272			*64, 74*
SaU 008	DS	0.2712	30	31				0.0501	2	2	*13*
SaU 094	DS	0.2656	28	29	0.0355	9	9	0.0493	2	2	*13, 26*
Shergotty	ES	0.1844	5	5	0.3728	28	28	0.0274	1	1	*13, 75*
Tissint	DS	0.2787	26	27	0.0272	2	2	0.0546	7	6	*7, 27*
Yamato 793605	IS	0.2140	28	28	0.1790	17	17				*76, 77*
Yamato 980459	DS	0.2670	11	12	0.0373	20	19				*78*
Zagami	ES	0.1843	6	6	0.3557	11	11	0.0273	1	1	*13, 58*

Type: ES = Enriched Shergottite, IS = Intermediate Shergottite, DS = Depleted Shergottite, OPX = Orthopyroxenite
Uncertainties are calculated by propagating the 2σ uncertainties in the age, the measured isotope ratio, and measured parent daugther ratios. This gives conservative minimum and maximum estimates fro the source composition. Note that these can be significantly assymetric.
The plus/minus value refers to the uncertainty on the last digit(s).

table S2. ^{147}Sm-^{143}Nd isotopic analyses of NWA 7635.

Sample	Sm ppm	Nd ppm	$^{147}Sm/^{144}Nd$	(2σ)	$^{143}Nd/^{144}Nd$	(2σ)
Whole Rock (F1)	**1.05**	**1.66**	**0.38327**	**77**	**0.517083**	**27**
Whole Rock 3 (F3)	1.06	1.70				
WR3-L1	39 ng	75 ng	0.31416	63	0.516068	13
WR3-L2	1 ng	2.7 ng	NA		NA	
WR3-L3 (HCl leach)	**20 ng**	**31 ng**	**0.38806**	**78**	**0.517120**	**34**
WR3-L4	8 ng	11 ng	0.44033	88	0.518282	25
WR3-L5	22 ng	29 ng	0.46628	93	0.518406	34
WR3-L6	9 ng	12 ng	0.48534	97	0.518528	25
Whole Rock 4 (F4)	1.06	1.83				
WR4-L	35 ng	67 ng	0.31632	63	0.516074	18
WR4-R	**59 ng**	**95 ng**	**0.37472**	**75**	**0.516956**	**27**
Olivine-rich fraction (F6)	1.29	2.05				
Olivine-L	35 ng	67 ng	0.31568	63	0.516010	34
Olivine-R	**59 ng**	**82 ng**	**0.43262**	**87**	**0.517840**	**27**
Pyroxene-rich fraction (F7)	0.98	1.55				
Pyroxene-L	17 ng	34 ng	0.30577	61	0.515946	34
Pyroxene-R	**29 ng**	**39 ng**	**0.44715**	**89**	**0.51816**	**34**
Weak acid leachates (n=4)[a]			**0.31399**	**153**	**0.516036**	**39**
Whole Rock HF step-wise dissolution (n=3)[b]			**0.46513**	**104**	**0.518408**	**39**
JNd-1 (n=27)					0.512115	26
UH Ames Nd (n=9)					0.511988	18
Caltech nNd-β (n=9)					0.511899	30

Concentrations for whole rock 3, whole rock 4, Olivine-rich fraction and Pyroxene-rich fraction are calculated by summing the total amount of Sm and Nd analyzed and dividing by sample weight pre-leaching. Absolute amounts of Sm and Nd analysed are listed in nanograms for each leachate (L) or residue (R). WR3-L2 contained too little REE to give a meaningful isotope analysis.
Rows in bold are used in the age regression.

[a]Integrated value for WR4 (leachate), WR3-L1, Olivine-L, and Pyroxene-L

[b]Integrated value for WR3-L4, WR3-L5, and WR3-L6

table S3. Descriptions and weights of NWA 7635 samples analyzed for radiogenic and cosmogenic isotopes.

Sample name	Sample material Leaching/Stepwise dissolution	Sample weight (g)	Analysis performed: Lu-Hf	Sm-Nd	Rb-Sr	Pb-Pb	Cosmogenic Nuclides
F1	bulk rock	0.1030	×	×			
F2	bulk rock						×
F3	>325 mesh bulk rock	0.0941					
F3-L1	0.5 M HNO3			×		×	
F3-L2	1.0 M HCl			×		×	
F3-L3	6.0 M HCl			×		×	
F3-L4	6.0 M HCl-0.2 M HF			×		×	
F3-L5	6.0 M HCl-2 M HF			×		×	
F3-L6	7.0 M HNO3 - 14M HF			×		×	
F4	>325 mesh bulk rock	0.0882					
F4-L	1.0 M HCl			×	×		
F4-R	Residue			×	×		
F5	hand picked plagioclase	0.00367					
F5-L	1.0 M HCl				×		
F5-R	Residue				×		
F6	olivine rich	0.0728					
F6-L	1.0 M HCl			×	×		
F6-R	Residue			×	×		
F7	pyroxene rich	0.0472					
F7-L	1.0 M HCl			×	×		
F7-R	Residue			×	×		

table S4. Laser ablation ICP-MS compositions of primary mineral phases in NWA 7635.

	Olivine	Pyroxene	Plagioclase	BIR-1G	2SD	Reference values*	2SD
Ca	4634	84928	83745	94260	800	95050 ± 1430**	
Sc	9.6	57.3	0.7	43.5	0.5	41 ± 2	
Ti	135	1030	135	5752	52	5532 ± 646	
V	28	255	2	314	5	338 ± 12	
Cr	1376	5392	22	399	4	403 ± 22	
Mn	6861	4111	71	1340	27	1417 ± 60	
Co	61.21	25.07	1.12	52.5	0.3	57 ± 2	
Ni	14	5	<12.85	166	5	190 ± 12	
Cu	15.1	6.0	0.9	124	2	132 ± 12	
Zn	401.5	77.3	14.5	73.9	1.8	86 ± 10	
Ga	1.37	5.22	27.68	16.1	0.3	17 ± 2	
Ge	0.95	1.63	<0.84	1.5	0.2	1.2 ± 0.1 **	
Rb	0.33	<0.169	<0.53	0.30	0.01	0.26 ± 0.1	
Sr	12.14	9.86	130.33	108	2	104 ± 4	
Y	3.38	5.81	0.50	14.7	0.2	13.3 ± 1.2	
Zr	1.10	1.02	0.24	13.7	0.4	12.9 ± 1.2	
Nb	<0.0215	0.02	0.10	0.55	0.04	0.48 ± 0.08	
Sn	0.61	0.65	1.74	1.52	0.11	0.84 ± 0.46	
Ba	5.40	1.37	0.62	6.56	0.27	6.3 ± 0.6	
La	0.06	0.01	0.01	0.61	0.01	0.60 ± 0.08	
Ce	0.20	0.09	0.07	1.91	0.07	1.90 ± 0.16	
Pr	0.04	0.02	0.02	0.38	0.01	0.36 ± 0.04	
Nd	0.30	0.22	0.11	2.45	0.17	2.3 ± 0.4	
Sm	0.11	0.17	0.09	1.14	0.11	1.1 ± 0.2	
Eu	0.03	0.06	0.45	0.54	0.03	0.51 ± 0.10	
Gd	0.29	0.47	0.13	1.72	0.07	1.6 ± 0.2	
Tb	0.07	0.11	0.02	0.36	0.03	0.32 ± 0.06	
Dy	0.54	0.89	0.11	2.48	0.18	2.3 ± 0.4	
Ho	0.12	0.21	0.02	0.56	0.04	0.51 ± 0.10	
Er	0.37	0.66	0.09	1.72	0.11	1.5 ± 0.2	
Tm	0.06	0.10	0.02	0.25	0.01	0.22 ± 0.04	
Yb	0.40	0.67	0.09	1.57	0.07	1.5 ± 0.2	
Lu	0.07	0.12	0.02	0.23	0.01	0.23 ± 0.04	
Hf	0.03	0.07	0.08	0.54	0.06	0.53 ± 0.12	

All data are in parts per million (ppm). * Values from (55) ** Values from (56)
2SD = 2 * standard deviation

table S5. ^{146}Sm-^{142}Nd isotopic analyses of NWA 7635.

Sample	Fraction	$\mu^{142}Nd$	$\mu^{145}Nd$	^{142}Ce interference (ppm)	^{144}Sm interference (ppm)	Spike/Sample molar ratio	Amount sample Nd analysed (ng)
NWA 7635	F3 L - Bulk	+108±10	-10±19	239.9±0.1	23.0±0.8	0.0449	67
	F3 R - Bulk	+88±12	+15±20	218.3±0.4	15.6±0.3	0.0795	95
	F4 L1 - Bulk	+80±11	-23±19	219.6±0.1	13.1±0.5	0.0703	75
	F4 L3 - Bulk	+107±22	+29±35	568.1±0.3	16.4±0.9	0.2182	31
	F4 L5 - Bulk	+93±20	-11±32	584.2±0.3	24.0±0.8	0.1729	29
	F6 L - Olivine Rich	+80±11	-1±20	213.7±0.1	15.3±0.3	0.0646	67
	F6 R - Olivine Rich	+82±12	+1±17	182.6±0.1	16.1±0.4	0.0347	82
	F7 L - Pyroxene Rich	+103±22	0±39	567.7±0.3	247.3±2.7	0.0739	34
	F7 R - Pyroxene Rich	+85±16	-1±30	473.5±0.3	17.8±1.3	0.0739	39
Average NWA 7635 (n=9)		+91.8±7.7	-0.3±10.0			Total sample:	519
Himalayan Garnet Schist #1	Inclusion free Garnet residue	-6±22	-21±55	537.4±0.4	70.5±1.6	0.0473	32
	Inclusion free Garnet Leach	+4±15	+5±29	67.9±0.2	3.7±0.4	0.0200	71
	Garnet residue	+12±14	+33±19	290.0±0.2	15.1±0.4	0.0026	108
	Garnet residue - Replicate 1	+3±12	+2±23	289.6±0.1	15.7±0.2	0.0026	112
	Garnet residue - Replicate 2	-2±13	-18±21	288.0±0.3	15.6±0.2	0.0026	114
	Garnet leach	+6±13	-7±18	1.8±0.1	-0.7±0.2	0.0031	116
	Garnet leach - Replicate 1	0±12	-5±22	2.0±0.1	0.5±0.2	0.0031	119
	Garnet leach - Replicate 2	-30±13	-23±19	2.1±0.1	0.8±0.2	0.0031	121
	Muscovite	+6±16	+13±31	139.5±0.3	22.5±0.4	0.2344	66
	Biotite	-11±16	-22±24	150.6±0.2	15.4±0.3	0.1956	82
	Whole Rock	+7±15	+12±26	61.6±0.2	2.1±0.6	0.1145	67
	Whole Rock - Replicate 1	+21±18	-17±26	60.8±0.2	0.9±0.4	0.1145	67
	Whole Rock - Replicate 2	-4±15	-22±26	60.8±0.2	1.1±0.3	0.1145	68
Average Himalayan Garnet Schist #1 (n=13)		0.0±9.9	-5.4±9.8			Total sample:	1144
Himalayan Garnet Schist #2	Inclusion free Garnet residue	-2±11	+2±17	38.7±0.1	3.0±0.8	0.0354	113
	Inclusion free Garnet residue -	-1±10	0±16	38.5±0.1	-1.3±0.3	0.0354	116
	Inclusion free Garnet Leach	+21±16	+19±32	169.8±0.2	12.6±1,2	0.2002	34
	Garnet residue	+13±6	+1±11	0.69±0.02	-0.8±0.4	0.0005	319
	Garnet residue - Replicate 1	-1±7	-12±12	0.72±0.02	-1.8±0.1	0.0005	316
	Garnet residue - Replicate 2	-12±6	-8±8	0.67±0.02	-1.6±0.2	0.0005	318
	Garnet residue - Replicate 3	-1±6	-7±11	0.68±0.02	-1.8±0.1	0.0005	320
	Garnet residue - Replicate 4	+12±6	+1±10	0.73±0.02	-1.4±0.1	0.0005	319
	Garnet residue - Replicate 5	+15±5	-13±9	0.74±0.03	-1.1±0.1	0.0005	327
	Garnet residue - Replicate 6	+17±7	-16±12	0.74±0.02	-1.4±0.1	0.0005	325
	Garnet leach	-14±10	+15±16	14.5±0.1	0.0±0.5	0.0170	113
	Garnet leach - Replicate 1	-11±10	-6±17	14.9±0.1	-1.3±0.3	0.0170	113
	Garnet leach - Replicate 2	-15±11	+21±15	14.7±0.1	-3.1±0.1	0.0170	114
	Felsic minerals	-7±9	0±16	56.2±0.1	4.9±0.6	0.0708	109
	Felsic minerals - Replicate 1	-10±8	0±13	56.4±0.1	4.3±0.5	0.0707	111
	Whole Rock	-9±8	-2±17	57.9±0.1	12.6±0.3	0.0605	139
	Whole Rock - Replicate 1	-12±8	+4±11	58.5±0.1	11.9±0.3	0.0605	145
Average Himalayan Garnet Schist #2 (n=17)		+0.8±6.0	+0.4±4.9			Total sample:	3350
External unspiked standards:							
Average Caltech nNd-β (n=5) run in session with NWA 7635		-4.3±7.3	-7.1±12.2	0.8±0.1	-2.3±0.5	Total sample:	309
Average JNdi-1 (n=7) run is session with Himalayan Schist #1		+5.1±7.5	+0.7±21.4	0.7±0.3	-0.9±0.7	Total sample:	283
Average JNdi-1 (n=7) run is session with Himalayan Schist #2		+4.4±10.3	+2.8±7.4	0.5±0.1	-0.9±0.3	Total sample:	757
Average JNdi-1 (n=6) run is session with NWA 6963 and LAR 12011		-2.4±10.3	-2.9±11.3	0.5±0.4	-0.7±0.6	Total sample:	250

Sample	Fraction	$\mu^{142}Nd$	$\mu^{145}Nd$	^{142}Ce interference (ppm)	^{144}Sm interference (ppm)	Spike/Sample molar ratio	Amount sample Nd analysed (ng)
NWA 6963	Bulk	-29±14	+5±12	40.8±0.1	25.0±0.2	0.0637	46
	Bulk - Replicate 1	-12±14	-1±13	40.9±0.1	25.1±0.2	0.0637	46
	Bulk - Replicate 2	-18±13	-13±14	40.9±0.1	24.3±0.2	0.0637	46
	Bulk - Replicate 3	-11±15	+10±14	40.4±0.1	25.3±0.2	0.0637	46
Average NWA 6963 (n=4)		-17.7±7.0	+0.6±6.6			Total sample:	184
LAR 12011	Bulk	-11±18	+30±12	33.1±0.1	22.0±0.2	0.0404	41
	Bulk - Replicate 1	-18±18	+11±15	32.9±0.1	20.1±0.2	0.0404	40
	Bulk - Replicate 2	-15±18	+17±12	32.0±0.1	20.9±0.3	0.0404	41
	Plagioclase	-17±19	+5±12	95.4±0.2	47.0±0.2	0.0510	49
	Plagioclase - Replicate 1	-9±18	+17±14	94.0±0.3	47.8±0.2	0.0510	50
	Pyroxene	-15±16	+2±12	158.0±0.1	43.4±0.2	0.0254	47
Average LAR 12011 (n=6)		-14.1±6.3	+13.7±11.1			Total sample:	268

table S6. Lu-Hf isotopic analyses of NWA 7635.

Sample name	Lu (ppm)	Hf (ppm)	$^{176}Lu/^{177}Hf$ 2σ	$^{176}Hf/^{177}Hf$ 2σ
F1 - Bulk Rock (not leached)	0.453	0.521	0.1200 ± 0.0003	0.287860 ± 0.000009
JMC 475 Hf, Wisconsin (n=3)				0.282176 ± 0.000007
Teledyne Hf (n=3)				0.282015 ± 0.000008

External reproducibility of $^{176}Hf/^{177}Hf$ is based on analyses of external standards listed above and the bracketing standard UH JMC 475 Hf giving $^{176}Hf/^{176}Hf = 0.282196 \pm 0.000009$ (2σ) (n=18).

table S7. Rb-Sr isotopic analyses of NWA 7635 maskelynite.

Sample name	Rb (ppm)	Sr (ppm)	$^{87}Rb/^{86}Sr$ 2σ (%)	$^{87}Sr/^{86}Sr$ 2σ (%)
F5 - maskelynite	0.19 ppm	429 ppm		
F5-L	0.25 (ng)	1228 (ng)	0.00058 ± 0.8	0.708434 ± 0.0026
F5-R	0.46 (ng)	347 (ng)	0.00385 ± 0.8	0.700032 ± 0.0026